



# World Scientific News

An International Scientific Journal

WSN 194 (2024) 102-120

EISSN 2392-2192

---

## **Influence of Electric and Magnetic Fields on the Thermal Performance of a Longitudinal Porous Convective-Radiative Fin with Temperature-dependent Internal Heat Generation using Homotopy Perturbation Method**

**Olamide Idris Fagbemi, Rafiu Olalekan Kuku\*, Suraju Aremu Oladosu**

Department of Mechanical Engineering, Lagos State University, Epe, Lagos, Nigeria

\*E-mail address: [rafiu.kuku@lasu.edu.ng](mailto:rafiu.kuku@lasu.edu.ng)

### **ABSTRACT**

High-performance equipment demands continuous advancement in technology, but excessive heat generation in these systems can lead to thermal-induced failure. This article adopted homotopy perturbation method to study the thermal behavior of a convective-radiative porous fin subjected to electric and magnetic field and with temperature-dependent internal heat generation. Utilizing the approximate analytical method to build a symbolic heat transfer model, the impacts of convective, radiative, and magnetic characteristics on the porous fin's thermal performance are examined. According to the study, increasing the porosity, convective, radiative, and magnetic characteristics of the fins cause an increase in heat transfer from the fin and its efficiency. The results of the homotopy perturbation method are verified by the results of numerical method and good agreement was established.

**Keywords:** Electric field, Magnetic Field, Homotopy Perturbation Method, Porous Fin, Heat transfer

## **1. INTRODUCTION**

Continuous technological improvement is necessary for high-performance equipment, but excessive heat generation in these systems might result in thermally-induced failure.

The pioneer work of Kiwan and Al-Nimr [1] has led to the development of various methods for analyzing the performance of porous fins in natural convection environments. Therefore, various researchers have been investigating the applications of porous fins in thermal systems, electronic components, and sensitive devices to improve heat transfer.

Such research works are evident in Kiwan [2-4], Gorla and Bakier [5], Kundu and Bhanja [6] and Kundu *et al.* [7], Taklifi *et al.* [8], Bhanja and Kundu [9] and Kundu *et al.* [10], Gorla *et al.* [11], Darvishi *et al.* [13] and Moradi *et al.* [14] and Ha *et al.* [15], Hoshyar *et al.* [16], Hatami and Ganji [17, 18], Rostamiyaan *et al.* [19], Ghasemi *et al.* [20]. These authors used numerous mathematical techniques for evaluating the performance of porous fins in natural convection situations. These include Adomian Decomposition, Spectral Collocation, Homotopy Perturbation, Homotopy Analysis, Least Square, variational iterative, and Differential Transformation methods are some other techniques. Oguntala *et al.* [21, 23-30, 32] and Sobamowo *et al.* [22, 31, 33-35] have worked extensively on porous fins under convective-radiative heat transfer and magnetic field using different approximate analytical and numerical methods.

However, as far as the authors are aware, no analysis of heat transfers in convective-radiative porous fins exposed to electric and magnetic fields with temperature-dependent internal heat generation has been done utilizing the homotopy perturbation method. Thus, the current study utilizes the homotopy perturbation method to investigate the thermal behavior of a convective-radiative porous fin in electric and magnetic fields with temperature-dependent internal heat generation. Utilizing the symbolic thermal model that developed, the effects of electromagnetic fields, internal heat generation, radiative and convective heat transfer on the porous fins are investigated.

## **2. PROBLEM FORMULATION**

As illustrated in Fig. 1, consider a straight porous fin with thickness  $t$  and length  $L$  that is subjected to a uniform magnetic field and is exposed on both faces to a convective environment at temperature. presuming that a single-phase fluid is saturated, the porous media is homogeneous, and isotropic.

Additionally, the physical characteristics of both solids and fluids are taken to be constant, with the exception of the fluid density variation, which could have an impact on the buoyancy term when the Boussinesq approximation is used. The temperature variation inside the fin is one-dimensional, meaning that it varies along the length only and remains constant over time, and there is no thermal contact resistance.

Fluid and porous media are locally in thermodynamic equilibrium in the domain, and surface radiative transfers and non-Darcian effects are minimal.

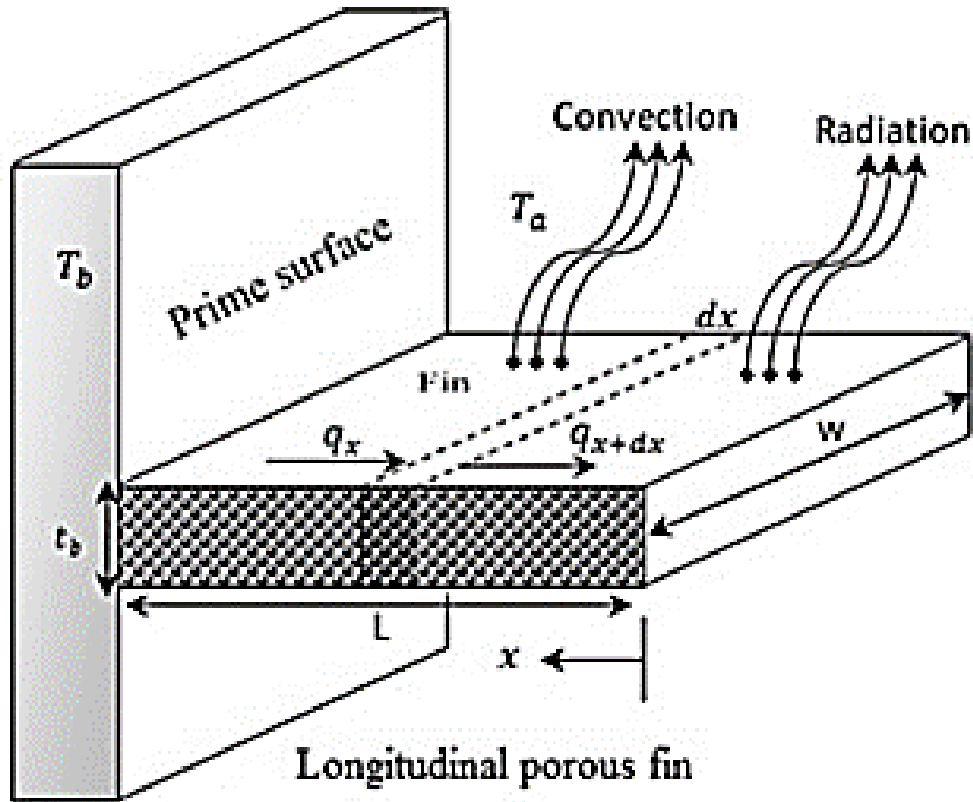


Fig. 1. Schematic of the convective-radiative longitudinal porous fin.

With respect to the aforementioned assumptions and Darcy's model, the thermal energy balance could be represented (Oguntala et al. (21, 23-30, 32) and Sobamowo et al. (22, 31, 33-35).

$$q_x - \left( q_x + \frac{\delta q}{\delta x} dx \right) + q(T) dx = \dot{m} c_p (T - T_a) + hP(1 - \varepsilon)(T - T_a) dx \tag{1}$$

$$+ \sigma \varepsilon P(T^4 - T_a^4) dx + \delta_b \zeta E^2 dx + \frac{\mathbf{J}_c \times \mathbf{J}_c}{\sigma} dx$$

where

$$\mathbf{J}_c = \sigma(\mathbf{E} + \mathbf{V} \times \mathbf{B}) \tag{2a}$$

The mass flow rate of the fluid through the porous material is given as

$$\dot{m} = \rho u(x) W dx \tag{3}$$

Adopting the Darcy's Model

$$u(x) = \frac{gK\beta}{\nu}(T - T_a) \tag{4}$$

Then, Equ. (1) becomes

$$q_x - \left( q_x + \frac{\delta q}{\delta x} dx \right) + q(T) dx = \frac{\rho c_p gK\beta}{\nu} (T - T_a)^2 dx + hP(1 - \varepsilon)(T - T_a) dx + \sigma \varepsilon P(T^4 - T_a^4) dx + \delta_b \zeta E^2 dx + \frac{\mathbf{J}_c \times \mathbf{J}_c}{\sigma} dx \tag{5}$$

As  $dx \rightarrow 0$ , Eq. (5) reduces

$$-\frac{dq}{dx} + q(T) = \frac{\rho c_p gK\beta}{\nu} (T - T_a)^2 + hP(1 - \varepsilon)(T - T_a) + \sigma \varepsilon P(T^4 - T_a^4) + \delta_b \zeta E^2 + \frac{\mathbf{J}_c \times \mathbf{J}_c}{\sigma} \tag{6}$$

Using Fourier's law of heat conduction, the rate of heat conduction in the fin is given by

$$q = -k_{eff} A_{cr} \frac{dT}{dx} \tag{7}$$

where

$$k_{eff} = \phi k_f + (1 - \phi) k_s$$

Based on Rosseland diffusion approximation, the radiation heat transfer rate is

$$q = -\frac{4\sigma A_{cr}}{3\beta_R} \frac{dT^4}{dx} \tag{8}$$

Therefore, the total rate of heat transfer is given by

$$q = -k_{eff} A_{cr} \frac{dT}{dx} - \frac{4\sigma A_{cr}}{3\beta_R} \frac{dT^4}{dx} \tag{9}$$

The substitution of Eq. (9) into Eq. (6), provides

$$\frac{d}{dx} \left( k_{eff} A_{cr} \frac{dT}{dx} + \frac{4\sigma A_{cr}}{3\beta_R} \frac{dT^4}{dx} \right) + q(T) = \frac{\rho c_p gK\beta}{\nu} (T - T_a)^2 + hP(1 - \varepsilon)(T - T_a) + \sigma \varepsilon P(T^4 - T_a^4) + \delta_b \zeta E^2 + \frac{\mathbf{J}_c \times \mathbf{J}_c}{\sigma} \tag{10}$$

Further simplification of Eq. (10) gives the governing differential equation for the fin as

$$\frac{d^2T}{dx^2} + \frac{4\sigma}{3\beta_R k_{eff}} \frac{d}{dx} \left( \frac{dT^4}{dx} \right) - \frac{\rho c_p g K \beta}{k_{eff} t v} (T - T_a)^2 - \frac{h(1-\varepsilon)}{k_{eff} t} (T - T_a) - \frac{\sigma \varepsilon}{k_{eff} t} (T^4 - T_a^4) - \frac{\delta_b \zeta E^2}{k_{eff} A_{cr}} - \frac{\mathbf{J}_c \times \mathbf{J}_c}{\sigma k_{eff} A_{cr}} + \frac{q(T)}{k_{eff} A_{cr}} = 0 \quad (11)$$

The boundary conditions are

$$\begin{aligned} x = 0, \quad \frac{dT}{dx} &= 0 \\ x = L, \quad T &= T_b \end{aligned} \quad (12)$$

But

$$\frac{\mathbf{J}_c \times \mathbf{J}_c}{\sigma} = \sigma B_o^2 u^2 \quad (13)$$

After substitution of Eq. (13) into Eq. (11),

$$\frac{d^2T}{dx^2} + \frac{4\sigma}{3\beta_R k_{eff}} \frac{d}{dx} \left( \frac{dT^4}{dx} \right) - \frac{\rho c_p g K \beta}{k_{eff} t v} (T - T_a)^2 - \frac{h(1-\varepsilon)}{k_{eff} t} (T - T_a) - \frac{\sigma \varepsilon (T^4 - T_a^4)}{k_{eff} t} - \frac{\delta_b \zeta E^2}{k_{eff} A_{cr}} - \frac{\sigma B_o^2 u^2}{k_{eff} A_{cr}} + \frac{q(T)}{k_{eff} A_{cr}} = 0 \quad (14)$$

The scenario taken into consideration in this work is one in which there is a slight temperature differential within the material when heat is transferred. In fact, this made it necessary to employ the fin's temperature-invariant thermal and physical capabilities. Furthermore, it has been shown that in this case, the term  $T^4$  can be written as a linear function of temperature. Consequently, we possess

$$T^4 = T_\infty^4 + 4T_\infty^3 (T - T_\infty) + 6T_\infty^2 (T - T_\infty)^2 + \dots \cong 4T_\infty^3 T - 3T_\infty^4 \quad (15)$$

Given that

$$q(T) = q_0 [1 + \lambda (T - T_\infty)]$$

when Eq. (15) is substituted into Eq. (14), then

$$\frac{d^2T}{dx^2} + \frac{16\sigma}{3\beta_R k_{eff}} \frac{d^2T}{dx^2} - \frac{\rho c_p g K \beta}{k_{eff} t v} (T - T_a)^2 - \frac{h(1-\varepsilon)}{k_{eff} t} (T - T_a) - \frac{4\sigma \varepsilon T_a^3 (T - T_a)}{k_{eff} t} - \frac{\sigma B_o^2 u^2}{k_{eff} A_{cr}} - \frac{\delta_b \zeta E^2}{k_{eff} A_{cr}} + \frac{q_0}{k_{eff} A_{cr}} [1 + \lambda (T - T_\infty)] = 0 \quad (16)$$

Using following dimensionless parameters in Eq. (17) into Eq. (16),

$$X = \frac{x}{L}, \theta = \frac{T - T_a}{T_b - T_a}, Ra = \frac{gk\beta(T_b - T_\infty)b}{\alpha\nu k_r}, Nc = \frac{pbh}{A_b k_{eff}}, E_b = \frac{\delta_b \zeta E^2 L^2}{k_{eff} A_{cr} (T_b - T_a)}$$

$$Rd = \frac{4\sigma_{st} T_\infty^3}{3\beta_R k_{eff}}, Nr = \frac{4\sigma_{st} b T_\infty^3}{k_{eff}}, H = \frac{\sigma B_0^2 u^2 L^2}{k_{eff} A_b (T_b - T_a)}. \tag{17}$$

we arrived at the dimensionless form of the governing Eq. (16) as

$$(1 + 4Rd) \frac{d^2\theta}{dX^2} - Ra\theta^2 - Nc(1 - \varepsilon)\theta - Nr\theta - H - E_b + M^2Q(1 + \gamma\theta) = 0 \tag{18}$$

or

$$\frac{d^2\theta}{dX^2} - \frac{Ra}{(1 + 4Rd)}\theta^2 - \frac{Nc(1 - \varepsilon)}{(1 + 4Rd)}\theta - \frac{Nr}{(1 + 4Rd)}\theta$$

$$- \frac{H}{(1 + 4Rd)} - \frac{E_b}{(1 + 4Rd)} + \frac{M^2Q}{(1 + 4Rd)}(1 + \gamma\theta) = 0 \tag{19}$$

Which can be written as

$$\frac{d^2\theta}{dX^2} - S_h\theta^2 - M_a^2\theta - H_m - E_m + M^2G(1 + \gamma\theta) = 0 \tag{20a}$$

where

$$S_h = \frac{Ra}{(1 + 4Rd)}, M^2 = \frac{Nc(1 - \varepsilon)}{(1 + 4Rd)} + \frac{Nr}{(1 + 4Rd)}, G = \frac{Q}{(1 + 4Rd)},$$

$$H_m = \frac{H}{(1 + 4Rd)}, E_m = \frac{E_b}{(1 + 4Rd)},$$

The dimensionless boundary conditions

$$X = 0, \quad \frac{d\theta}{dX} = 0$$

$$X = 1, \quad \theta = 1 \tag{20b}$$

### 3. METHOD OF SOLUTION BY HOMOTOPY PERTURBATION METHOD

Developing a closed-form solution for the aforementioned non-linear problem (19) is exceedingly challenging. As a result, one has to use either numerical method, semi-numerical method, or approximate analytical method. The homotopy perturbation approach is employed in this paper to solve the equation. Homotopy perturbation method has so quickly gained popularity in the field of approximating analytical solutions to linear and nonlinear differential equations, as seen by the numerous engineering and scientific research publications that have featured it. A pantograph equation, an integro-differential equation, fractional differential equations, difference equations, differential-difference equations, and differential equations can all be solved using this approximative analytical method. Without using discretization, linearization, closure, restrictive assumptions, perturbation, approximations, round-off error, or linearization, which could require enormous amounts of computational work, it solves nonlinear integral and differential equations. Differential or algebraic equations need not need a tiny parameter, as is the case with other conventional perturbation techniques. For the solution of non-linear equations, it offers highly accurate approximations [36–40].

#### 3. 1. The basic idea of homotopy perturbation method

The basic idea, principle and application of the method can be found in He [36-40] and Sobamowo et al. [31].

#### 3. 2. Application of the homotopy perturbation method to the present problem

According to homotopy perturbation method (HPM), one can construct an homotopy for Eq.

$$(19) \text{ as } H(\theta, p) = (1-p) \left[ \frac{d^2\theta}{dX^2} \right] + p \left[ \frac{d^2\theta}{dX^2} - S_h \theta^2 - M^2 \theta - E_m - H_m + M^2 G(1 + \gamma \theta) \right] \quad (21)$$

where  $p \in [0, 1]$  is an embedding parameter. For  $p = 0$ , and  $p = 1$ , we have

$$\theta(X, 0) = \theta_0(X) \quad , \quad \theta(X, 1) = \theta_0(X) \quad (22)$$

Note that when  $p$  increases from 0 to 1,  $\theta(X, p)$  varies from  $\theta_0(X)$  to  $\theta_0(X)$ . Supposing that the solution of Eq.(19) can be expressed in a series in  $p$ :

$$\theta(X) = \theta_0(X) + p\theta_1(X) + p^2\theta_2(X) + p^3\theta_3(X) + \dots = \sum_{i=0}^n p^i \theta_i(X) \quad (23)$$

On substituting Eqs. (23) and into Eq.(21) and expanding the equation and collecting all terms with the same order of  $p$  together, the resulting equation appears in form of polynomial in  $p$ . On equating each coefficient of the resulting polynomial in  $p$  to zero, we arrived at a set of differential equations and the corresponding boundary conditions as

$$p^0: \frac{d^2\theta_0}{dX^2}(X) = 0, \quad \theta_0(0) = 1 \quad \theta'_0(1) = 0 \quad (24)$$

$$p^1: \frac{d^2\theta_1}{dX^2} + M^2G\gamma\theta_0 - S_h\theta_0^2 - M^2\theta_0 - H_m - E_m + M^2G = 0, \quad \theta_1(0) = 0 \quad \theta'_1(1) = 0 \quad (25)$$

$$p^2: \frac{d^2\theta_2}{dX^2} + M^2G\gamma\theta_1 - S_h\theta_0\theta_1 - M^2\theta_1 = 0, \quad \theta_2(0) = 0 \quad \theta'_2(1) = 0 \quad (26)$$

$$p^3: \frac{d^2\theta_3}{dX^2} + M^2G\gamma\theta_2 - S_h\theta_1^2 - 2S_h\theta_0\theta_2 - M^2\theta_1 = 0, \quad \theta_3(0) = 0 \quad \theta'_3(1) = 0 \quad (27)$$

$$p^4: \frac{d^2\theta_4}{dX^2} - M^2\theta_3 - 2S_h\theta_1\theta_2 - 2S_h\theta_0\theta_3 + M^2G\gamma\theta_3 = 0, \quad \theta_4(0) = 0 \quad \theta'_4(1) = 0 \quad (28)$$

On solving the above Eqs. (24-28), we arrived at

$$\theta_0(X) = 1 \quad (29)$$

$$\theta_1(X) = \frac{[M^2[1-G(1+\gamma)] + H_m + E_m + S_h]}{2}(X^2 - 1) \quad (30)$$

$$\theta_2(X) = \frac{[M^2[1-G(1+\gamma)] + H_m + E_m + S_h](M^2 + 2S_h - M^2G\gamma)}{24}(X^4 - 6X^2 + 5) \quad (31)$$



$$\theta_3(X) = \left[ \begin{array}{l} \left( S_h \left( \frac{[M^2[1-G(1+\gamma)]+H_m+E_m+S_h]}{2} \right)^2 + \frac{(M^2+2S_h-M^2G\gamma) \left( \frac{[M^2[1-G(1+\gamma)]+H_m+E_m+S_h]}{2} \right) (M^2+2S_h-M^2G\gamma)}{2} \right) \frac{X^6}{30} - \\ \left( 2S_h \left( \frac{[M^2[1-G(1+\gamma)]+H_m+E_m+S_h]}{2} \right)^2 + \frac{(M^2+2S_h-M^2G\gamma) \left( \frac{[M^2[1-G(1+\gamma)]+H_m+E_m+S_h]}{2} \right) (M^2+2S_h-M^2G\gamma)}{2} \right) \frac{X^4}{12} + \\ \left( S_h \left( \frac{[M^2[1-G(1+\gamma)]+H_m+E_m+S_h]}{2} \right)^2 + \frac{5(M^2+2S_h-M^2G\gamma) \left( \frac{[M^2[1-G(1+\gamma)]+H_m+E_m+S_h]}{2} \right) (M^2+2S_h-M^2G\gamma)}{2} \right) \frac{X^2}{2} - \\ \left( \frac{11}{30} S_h \left( \frac{[M^2[1-G(1+\gamma)]+H_m+E_m+S_h]}{2} \right)^2 + \frac{61(M^2+2S_h-M^2G\gamma) \left( \frac{[M^2[1-G(1+\gamma)]+H_m+E_m+S_h]}{2} \right) (M^2+2S_h-M^2G\gamma)}{360} \right) \end{array} \right] \quad (32)$$

The definition of HPM provides

$$\theta(X) = \theta_0(X) + p\theta_1(X) + p^2\theta_2(X) + p^3\theta_3(X) + p^4\theta_4(X) + \dots \quad (33)$$

Therefore, setting  $p = 1$ , results in the approximation solution of Eq. (33)

$$\theta(X) = \lim_{p \rightarrow 1} \theta(X) = \theta_0(X) + \theta_1(X) + \theta_2(X) + \theta_3(X) + \theta_4(X) + \dots \quad (34)$$

On substituting Eq. (30-33), we have

$$\theta(X) = 1 - \frac{[M^2[1-G(1+\gamma)] + H_m + E_m + S_h]}{2}(1-X^2) + \frac{[M^2[1-G(1+\gamma)] + H_m + E_m + S_h](M^2 + 2S_h - M^2G\gamma)}{24}(X^4 - 6X^2 + 5) + \left[ \begin{aligned} & \left( \frac{S_h \left( \frac{[M^2[1-G(1+\gamma)] + H_m + E_m + S_h]}{2} \right)^2}{\frac{(M^2 + 2S_h - M^2G\gamma)}{12} \left( \frac{[M^2[1-G(1+\gamma)] + H_m + E_m + S_h](M^2 + 2S_h - M^2G\gamma)}{2} \right)} \right) \frac{X^6}{30} - \\ & \left( \frac{2S_h \left( \frac{[M^2[1-G(1+\gamma)] + H_m + E_m + S_h]}{2} \right)^2}{\frac{(M^2 + 2S_h - M^2G\gamma)}{2} \left( \frac{[M^2[1-G(1+\gamma)] + H_m + E_m + S_h](M^2 + 2S_h - M^2G\gamma)}{2} \right)} \right) \frac{X^4}{12} + \\ & \left( \frac{S_h \left( \frac{[M^2[1-G(1+\gamma)] + H_m + E_m + S_h]}{2} \right)^2}{\frac{5(M^2 + 2S_h - M^2G\gamma)}{12} \left( \frac{[M^2[1-G(1+\gamma)] + H_m + E_m + S_h](M^2 + 2S_h - M^2G\gamma)}{2} \right)} \right) \frac{X^2}{2} - \\ & \left( \frac{\frac{11}{30} S_h \left( \frac{[M^2[1-G(1+\gamma)] + H_m + E_m + S_h]}{2} \right)^2}{\frac{61(M^2 + 2S_h - M^2G\gamma)}{360} \left( \frac{[M^2[1-G(1+\gamma)] + H_m + E_m + S_h](M^2 + 2S_h - M^2G\gamma)}{2} \right)} \right) \end{aligned} \right] + \dots \tag{35}$$

#### 4. RESULTS AND DISCUSSION

The developed thermal model in Eq. (35) are coded and simulated in MATLAB. Firstly, the results of the HPM need to be verified before, it can be used for parametric studies. Therefore, the Runge-Kutta fourth-order method is utilized to numerically solve the governing differential equation in order to verified the homotopy perturbation method employed in this work. As seen in Table 1, the results of the numerical approach are displayed. The Table suggests that the HPM is quite precise and has excellent agreement with the numerical technique.

**Table 1.** Comparison of results

| X   | Numerical | Present (HPM) |
|-----|-----------|---------------|
| 0.0 | 0.886794  | 0.886819      |
| 0.2 | 0.891243  | 0.891257      |
| 0.4 | 0.904595  | 0.904614      |
| 0.6 | 0.927017  | 0.927026      |
| 0.8 | 0.958709  | 0.958715      |
| 1.0 | 1.000000  | 1.000000      |

The effects of porosity or porous parameter on the temperature distribution in the porous fin are displayed in Fig. 2. The temperature in the fin drops more quickly as the porosity parameter increases, as shown in the figures, and the rate of heat transfer (the convective-radiative heat transfer) through the fin increases as the temperature decreases quickly. When the porosity parameter increases, the Raleigh number increases as well, increasing the permeability of the porous fin and the working fluid's ability to pass through its pores. This increases the effect of buoyancy force, which causes the fin to convect more heat, and the fin's temperature drops quickly. The fin exhibits improved heat transfer and greater thermal performance. As convective heat transfer increases, fin porosity increases and hence improves fin efficiency.

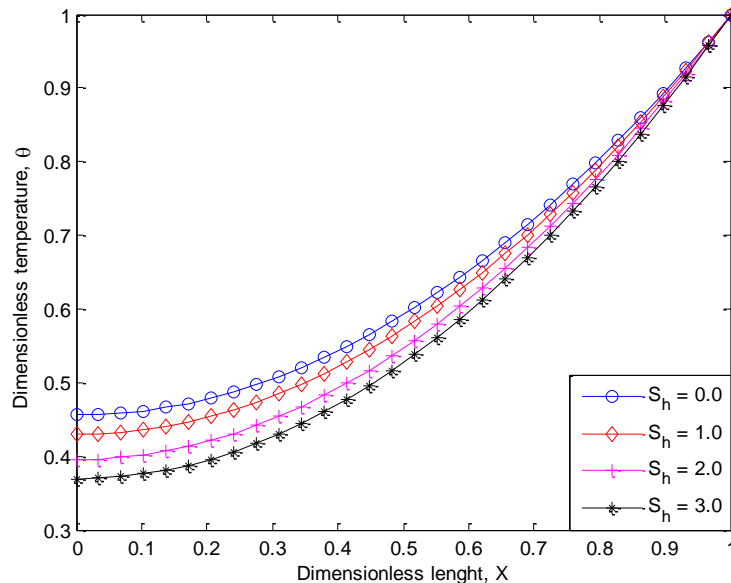


**Fig. 2.** Dimensionless temperature distribution in the fin parameters for varying porous parameter

The effects of the conduction-convection parameter on the fin's temperature distribution are depicted in Figure 3. The graphic shows that the rate of heat transfer through the fin increases as the conduction-convection parameter increases. This is because the fin's temperature lowers more quickly, resulting in a steeper fin that reflects high base heat flow rates. The profile with the steepest temperature gradient is one with a lower conduction-convection term value. However, its value is significantly higher due to its lower thermal conductivity than the other profiles' values of  $N_c$ , which results in a lower heat-transfer rate. This demonstrates that the fin's thermal performance or efficiency is preferred at low convective parameter values because the goal (high effective utilization of the fin) is to reduce the temperature drop along the fin length, where  $T=T_b$  everywhere is the ideal condition. It is important to note that a small number for  $M$  indicates a relatively short and thick fin with low thermal conductivity, whereas a high value for  $M$  indicates a long fin or fin with low thermal conductivity. Very lengthy fins should be avoided in practice since the fin's thermal performance or efficiency is best at low convective fin parameter values.

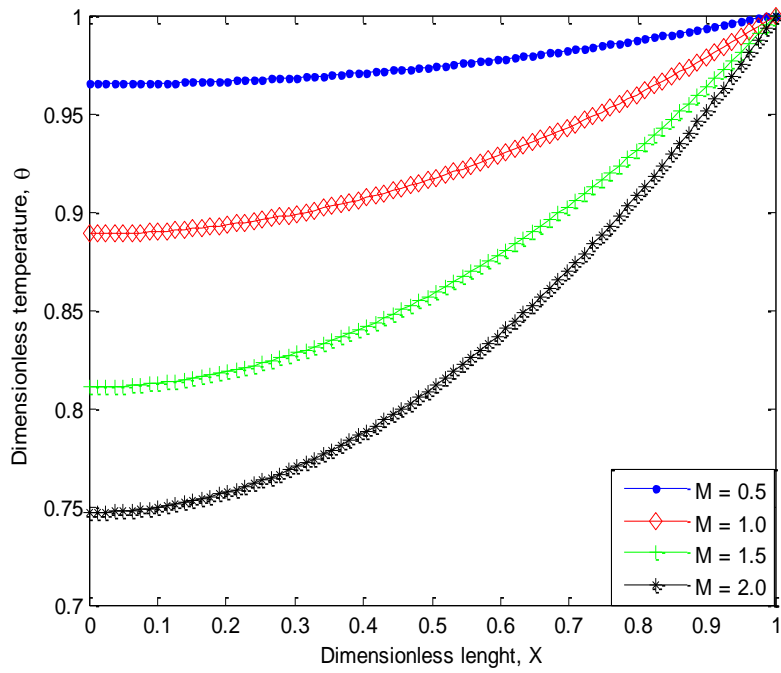


**Fig. 3.** Dimensionless temperature distribution in the fin parameters for varying convection-conduction parameter

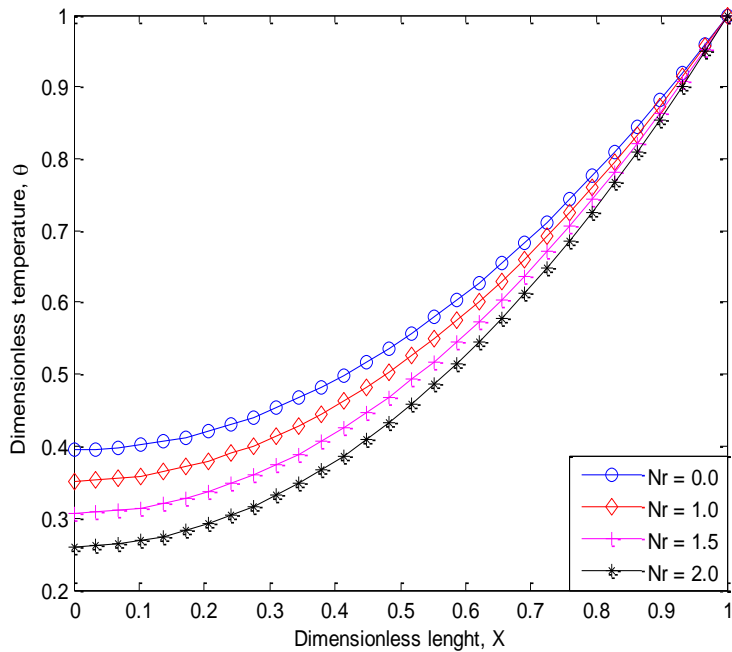


**Fig. 4.** Dimensionless temperature distribution in the fin parameters for varying radiation-conduction parameter

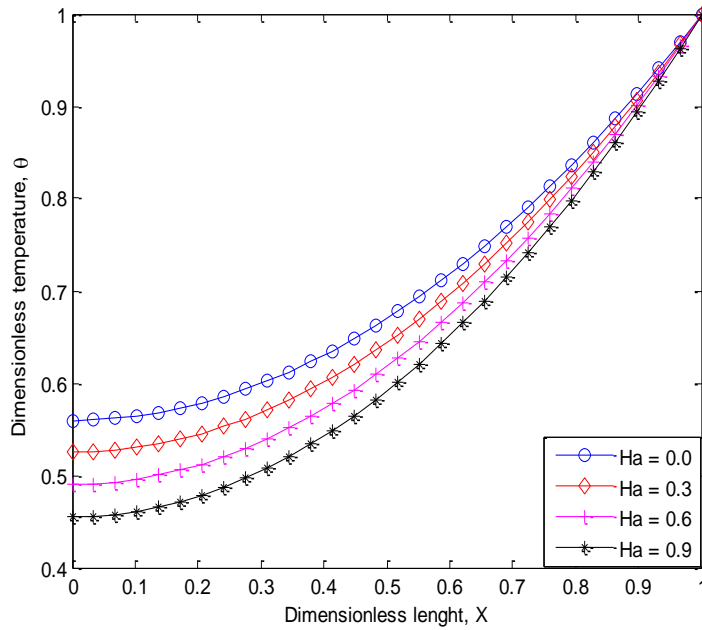


**Fig. 5.** Dimensionless temperature distribution in the fin parameters for varying magnetic parameter

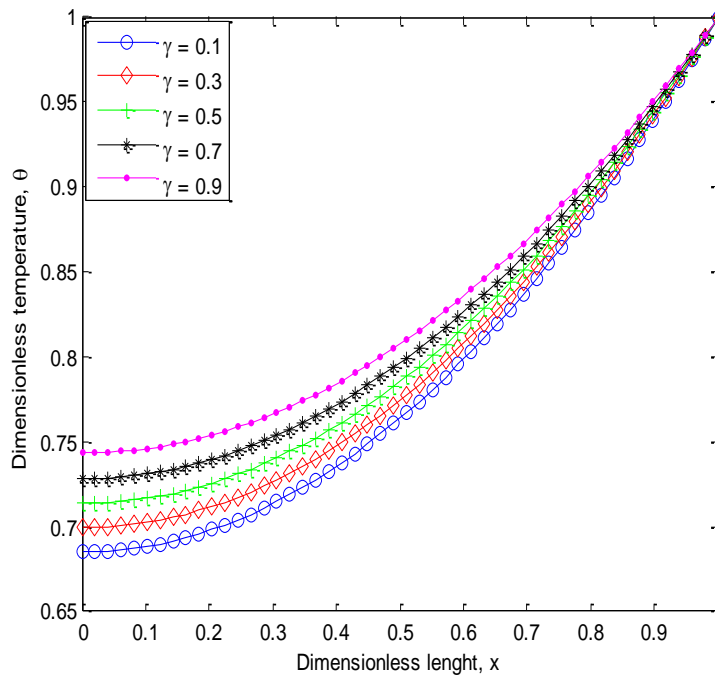


**Fig. 6.** Dimensionless temperature distribution in the fin parameters for varying internal heat generation parameters,

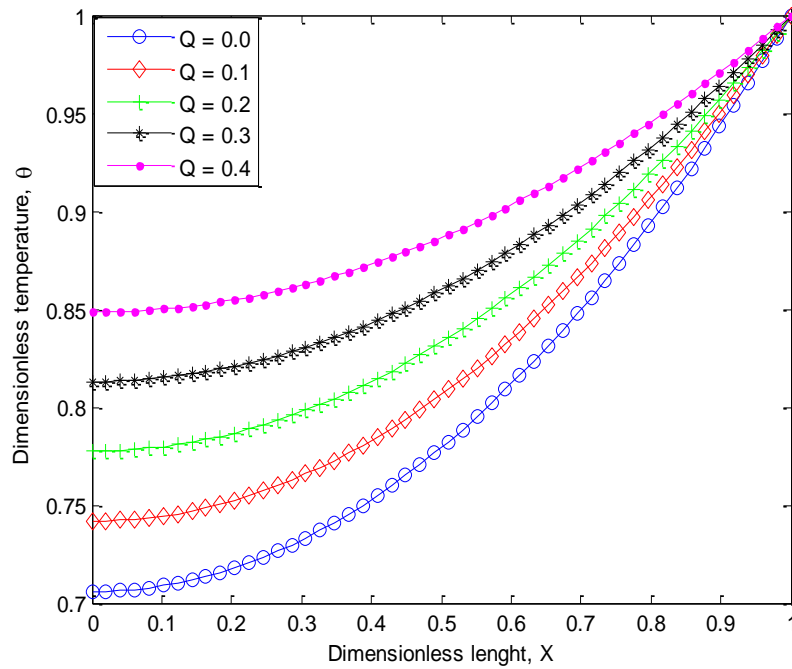


**Fig. 7.** The fin temperature profiles for varying values of internal heat generation parameter,  $Q$

Figure 4 illustrates the impact of the conduction-radiation parameter. The graphic illustrates how the rate of heat transfer through the fin increases with an increase in the conduction-radiation parameter. Figure 5 illustrates how the temperature distribution in the porous fin is affected by the magnetic parameter, or Hartman number. The figure illustrates how enhanced heat transfer via porous fins can be achieved by the induced magnetic field within the fin. This same trend was found in the impact of electric field on the fin's thermal performance. Therefore, figures 2–6 demonstrate how increasing the fin's porosity, convective, radiative, and magnetic characteristics speeds up heat transfer from the fin and raises its efficiency as a result. While Figure 6 illustrates the impacts of a temperature-dependent internal heat production parameter on the temperature distribution in the fin, Figure 7 show the effects of an internal heat generation parameter on the temperature distribution in the porous fin. According to the figures, the temperature gradient of the fins diminishes as the internal heat generating parameters increase, which in turn causes a drop in the fin's rate of heat transmission. It should be noted that because of their low heat conductivity and high surface area when in contact with the cooling fluid, fins made of porous material function better and weigh far less than fins made of solid metal.

## 5. CONCLUSION

This work adopted the homotopy perturbation approach to assess the thermal behavior of a convective-radiative porous fin subjected to electric and magnetic field and with temperature-

dependent internal heat generation. The effects of different factors on the thermal performance of the porous fin were examined using the established symbolic heat transfer models. It was found that increasing the electric field, magnetic field, porosity, convective-radiative heat transfer parameters cause increase in the rate of heat transfer from the base of the fin. Moreover, an increase in the internal heat generation and the thermal conductivity parameters cause the fin temperature to increase. The work will help in the better design of the passive device especially in an electromagnetic environment.

### Nomenclature

A cross sectional area of the fins  
 $A_b$  porous fin base area  
 $A_s$  porous fin surface area  
 $B_0$  Magnetic field intensity  
 $c_p$  specific heat of the fluid passing through porous fin  
 $Da$  Darcy number  
 $E$  electric field  
 $g$  gravity constant  
 $h$  heat transfer coefficient over the fin surface  
 $h_b$  heat transfer coefficient at the base of the fin  
 $J$  conduction current intensity  
 $J_c$  Conduction current intensity  
 $K$  permeability of the porous fin  
 $k$  thermal conductivity of the fin material  
 $k$  Thermal conductivity  
 $k_b$  thermal conductivity of the fin material at the base of the fin  
 $k_{eff}$  effective thermal conductivity ratio  
 $k_r$  Thermal conductivity ratio  
 $L$  Length of the fin, m  
 $M$  dimensionless thermo-geometric parameter  
 $m$  mass flow rate of fluid passing through porous fin  
 $Nu$  Nusselt number  
 $P$  perimeter of the fin  
 $P$  Fin perimeter (m)  
 $Q$  dimensionless heat transfer rate per unit area  
 $q$  internal heat generation  
 $q_b$  heat transfer rate per unit area at the base  
 $Q_s$  dimensionless heat transfer rate the base  
 $R_s$  Surface-ambient radiation parameter  
 $Ra$  Rayleigh number  
 $Ra^*$  Modified Rayleigh number  
 $Rd$  Radiation-conduction parameter  
 $S_h$  Porosity parameter  
 $t$  thickness of the fin  
 $T$  fin temperature  
 $T_a$  ambient temperature  
 $T_b$  Temperature at the base of the fin  
 $u$  Axial velocity  
 $v$  average velocity of fluid passing through  
 $w$  width of the fin  
 $x$  axial length measured from fin tip  
 $X$  dimensionless length of the fin  
 $W$  width of the fin

### Greek Symbols

- $\alpha$  Thermal diffusivity  
 $\beta_R$  Rosseland extinction coefficient  
 $\varepsilon$  Emissivity  
 $\mu$  Dynamic viscosity  
 $\nu$  Kinematic viscosity  
 $\sigma$  Electric conductivity  
 $\sigma_{st}$  Stefan–Boltzmann constant  
 $\rho$  Density of the fluid  
 $\rho_e$  Electrical density

### References

- [1] S. Kiwan, A. Al-Nimr. Using Porous Fins for Heat Transfer Enhancement. *ASME Journal of Heat Transfer* 2001; 123: 790–5
- [2] S. Kiwan, Effect of radiative losses on the heat transfer from porous fins. *International Journal of Thermal Sciences* 46 (2007a) 1046-1055
- [3] S. Kiwan. Thermal analysis of natural convection porous fins. *Transport in Porous Media* 67 (2007b), 17-29.
- [4] S. Kiwan, O. Zeitoun, Natural convection in a horizontal cylindrical annulus using porous fins. *International Journal of Numerical Methods for Heat and Fluid Flow* 18 (5) (2008), 618-634.
- [5] R. S. Gorla, A. Y. Bakier. Thermal analysis of natural convection and radiation in porous fins *International Communications in Heat and Mass Transfer* 38 (2011), 638-645.
- [6] B. Kundu, D. Bhanji. An analytical prediction for performance and optimum design analysis of porous fins. *International Journal of Refrigeration* 34 (2011), 337-352.
- [7] B. Kundu, D. Bhanja, K. S. Lee. A model on the basis of analytics for computing maximum heat transfer in porous fins. *International Journal Heat and Mass Transfer* 55 (25-26) (2012), 7611-7622.
- [8] A. Taklifi, C. Aghanajafi, H. Akrami. The effect of MHD on a porous fin attached to a vertical isothermal surface. *Transport in Porous Media* 85 (2010), 215–31.
- [9] D. Bhanja, B. Kundu. Thermal analysis of a constructal T-shaped porous fin with radiation effects. *International Journal of Refrigeration* 34 (2011), 1483–96.
- [10] B. Kundu, Performance and optimization analysis of SRC profile fins subject to simultaneous heat and mass transfer. *International Journal Heat and Mass Transfer* 50 (2007), 1545-1558
- [11] R. Gorla, R.S., Darvishi, M. T. Khani, F. Effects of variable Thermal conductivity on natural convection and radiation in porous fins. *International Communications in Heat and Mass Transfer* 38 (2013), 638-645



- [12] S. Saedodin, M. Shahbabaie. Thermal Analysis of Natural Convection in Porous Fins with Homotopy Perturbation Method (HPM). *Arabian Journal for Science and Engineering* (2013), 38: 2227–2231
- [13] M. T. Darvishi, R. Gorla, R.S., Khani, F., Aziz, A.-E. Thermal performance of a porous radial fin with natural convection and radiative heat losses. *Thermal Science*, 19 (2) (2015), 669-678.
- [14] A. Moradi, T. Hayat and Alsaedi, A. Convective-radiative thermal analysis of triangular fins with temperature-dependent thermal conductivity by DTM. *Energy Conversion and Management* 77 (2014), 70–77
- [15] H. Ha, Ganji D. D and Abbasi M. Determination of Temperature Distribution for Porous Fin with Temperature-Dependent Heat Generation by Homotopy Analysis Method. *Journal of Applied Mechanics And Engineering*, 4 (1) (2005).
- [16] H. A. Hoshyar, I. Rahimipetroudi, D. D. Ganji, A. R. Majidian. Thermal performance of porous fins with temperature-dependent heat generation via Homotopy perturbation method and collocation method. *Journal of Applied Mathematics and Computational Mechanics*. 14 (4) (2015), 53-65.
- [17] M. Hatami, D. D. Ganji. Thermal performance of circular convective-radiative porous fins with different section shapes and materials. *Energy Conversion and Management*, 76 (2013), 185–193
- [18] M. Hatami, D. D. Ganji. Thermal behavior of longitudinal convective–radiative porous fins with different section shapes and ceramic materials (SiC and Si<sub>3</sub>N<sub>4</sub>). *Ceramics International Journal*, 40 (2014), 6765–6775
- [19] Y. Rostamiyan, D. D. Ganji, I. R. Petroudi, and M. K. Nejad. Analytical Investigation of Nonlinear Model Arising in Heat Transfer Through the Porous Fin. *Thermal Science*. 18 (2) (2014), 409-417.
- [20] S. E. Ghasemi, P. Valipour, M. Hatami, D. D. Ganji. Heat transfer study on solid and porous convective fins with temperature-dependent heat - generation using efficient analytical method. *Journal of Central South University* 21 (2014), 4592–4598
- [21] G. A. Oguntala, M. G. Sobamowo, A. A. Yinusa. Transient analysis of functionally graded material porous fin under the effect of Lorentz force using the integral transform method for improved electronic packaging. *Heat transfer*, 2020, 1-18.
- [22] M. G. Sobamowo, G. Oguntala, A. A. Yinusa. Nonlinear Transient Thermal Modeling and Analysis of a Convective-Radiative Fin with Functionally Graded Material in a Magnetic Environment. *Modelling and Simulation in Engineering*, Article ID 7878564, 2019, 16 pages.
- [23] G. Oguntala, M. G. Sobamowo, R. Abd-Alhameed, S. Jones. Efficient iterative method for the investigation of convective-radiative porous fin with internal heat generation under a uniform magnetic field. *International Journal of Applied and computational mathematics*. 5(1), 1-9.
- [24] G. Oguntala, M. G. Sobamowo, R. Abd-Alhameed (2019). Numerical analysis of transient response of convective-radiative cooling fin with convective tip under

- magnetic field for reliable thermal management of electronic systems. *Thermal Science and Engineering Progress*. 9, 289-298.
- [25] G. Oguntala, M. G. Sobamowo, R. Abd-Alhameed, J. Noras, (2019). Numerical Study of Performance of Porous Fin Heat Sink of Functionally Graded Material for Improved Thermal Management of Consumer Electronics. *IEEE Transactions on Components, Packaging, and Manufacturing Technology*. 99 1271-1283.
- [26] G. Oguntala, M. G. Sobamowo, R. Abd-Alhameed, J. Noras, (2019). Investigation of Simultaneous Effects of Surface Roughness, Porosity and Magnetic Field of Rough Porous Micro-Fin under a Convective-Radiative Heat Transfer for Improved Electronic Cooling of Microprocessors. *IEEE Transactions on Components, Packaging, and Manufacturing Technology*. 9(2), 235-246
- [27] G. A. Oguntala, I. Danjuma, M. G. Sobamowo, R. Abd-Alhameed and J. Noras. Nonlinear Thermal Analysis of a Convective-Radiative Longitudinal Porous Fin of Functionally Graded Material for Efficient Cooling of Consumer Electronics International Journal of Ambient Energy. *International Journal of Ambient Energy*. 2019. doi.org/10.1080/01430750.2019.1636863
- [28] G. A. Oguntala, R. Abd-Alhameed and M. G. Sobamowo. On the Effect of Magnetic Field on Thermal Performance of Convective-radiative fin with Temperature-dependent Thermal Conductivity. *Karbala International Journal of Modern Science* 4, 1-11.
- [29] G. A. Oguntala, M. G. Sobamowo, A. A. Yinusa and R. Abd-Alhameed. Application of Approximate Analytical Technique Using the Homotopy Perturbation Method to Study the Inclination Effect on the Thermal Behavior of Porous Fin Heat Sink. *Mathematical and Computational Applications* 23(4): 1-12.
- [30] G. A. Oguntala, R. Abd-Alhameed, M. G. Sobamowo and I. Danjuma. Performance, Thermal Stability and Optimum Design Analyses of Rectangular Fin with Temperature-Dependent Thermal Properties and Internal Heat Generation. *Journal of Computational Applied Mechanics*. Vol. 49(1). 37-43
- [31] M. G. Sobamowo, O. A. Adeleye and A. A. Yinusa. Analysis of convective-radiative porous fin with temperature-dependent internal heat generation and magnetic using homotopy perturbation method. *Journal of Computational and Applied Mechanics*. Vol. 12(2), 127-145
- [32] G. A. Oguntala and M. G. Sobamowo. Galerkin's Method of weighted residual for a convective straight fin with temperature-dependent conductivity and internal heat generation. *International Journal of Engineering and Technology*, 6(12) (2016), 433-442.
- [33] M. G. Sobamowo. Thermal analysis of longitudinal fin with temperature-dependent properties and internal heat generation using Galerkin's method of weighted residual. *Applied Thermal Engineering*, 99(2016), 1316-1330.
- [34] M.G. Sobamowo, O.M. Kamiyo, O.A. Adeleye. Thermal performance analysis of a natural convection porous fin with temperature-dependent thermal conductivity and internal heat generation. *Thermal Science and Engineering Progress* 1 (2017) 39–52.

- [35] M.G. Sobamowo. Singular perturbation and differential transform methods to two-dimensional flow of nanofluid in a porous channel with expanding/contracting walls subjected to a uniform transverse magnetic field. *Thermal Science and Engineering Progress* 4 (2017), 71-8
- [36] J. H. He. Homotopy Perturbation Technique. *Computer Methods in Applied Mechanics and Engineering*, 178, 257-262, 1999
- [37] J. H. He. New Interpretation of Homotopy Perturbation Method. *International Journal of Modern Physics B*, 20, 2561-2568, 2006.
- [38] J. H. He. A Coupling Method of Homotopy Technique and Perturbation Technique for Nonlinear Problems. *International Journal of Non-Linear Mechanics*, 35, 37-43, 2000.
- [39] J. H. He. Some Asymptotic Methods for Strongly Nonlinear Equations. *International Journal of Modern Physics B*, 20, 1141-1199, 2006.
- [40] J. H. He. New Perturbation Technique Which Is Also Valid for Large Parameters. *Journal of Sound and Vibration*, 229, 1257-1263, 2000